To be published in International Journal of Steel Structures
Date accepted: 30/12/2019
DOI: 10.1007/s13296-020-00306-8

Dynamic instability analysis of axially compressed castellated columns

Jin-song Lei[a,b], Boksun Kim[c], Long-yuan Li[c]

a) College of Civil Engineering and Architecture, Southwest University of Science and Technology, Mianyang 621010, China (leijinsong@swust.edu.cn)
b) Shock and Vibration of Engineering Materials and Structures Key Laboratory of Sichuan Province, Southwest University of Science and Technology, Mianyang 621010, China
c) School of Engineering, University of Plymouth, Plymouth PL4 8AA, UK

Abstract – This paper presents an analytical study on the dynamic instability of castellated columns subjected to axial excitation loading. By assuming the instability modes, the kinetic energy and strain energy of the columns and the loss of the potential of the axially applied load are evaluated, from which the mass matrix, stiffness matrix, and geometric stiffness matrix of the system are derived. These matrices are then used for deriving dynamic equations and carrying out the analysis of dynamic instability of castellated columns by using Bolotin's method. The analytical expression for determining the critical excitation frequency of the columns is derived, which takes account for not only the shear influence of web openings but also the rotary inertia effect on the transverse vibration of the columns. Numerical examples are also provided for illustrating the dynamic instability behaviour of castellated columns when subjected to axial excitation loading. The results show that the consideration of the shear effect in castellated columns results in a shaft of the dynamic instability zone to low frequency side and a reduction of the width of the dynamic instability zone. The shear effect on the dynamic instability zone becomes more significant in the short column than in the long column, and in the wide flange column than in the narrow flange column.

Keywords: Dynamic instability; vibration; buckling; castellated column; shear effect; inertia effect.

1. Introduction

Castellated beams and columns have been widely used in structures and steel buildings. Compared to traditional I-section structural members, castellated structural members can have large section depth and thus have great flexural capacity while they are bent about their major axis and large flexural buckling resistance when they are subjected to axial loading. The second advantage of using castellated members in buildings is the light in weight, which not only can save material cost but also reduce the load on the columns and foundation. The main dimness of the castellated members, however, is the weak shear rigidity due to the openings in the web, which can affect the performance of the members in vibration and bending, as well as their resistance against buckling.

The economical and structural advantages of castellated members have prompted many researchers to investigate the behaviour and performance of such structures. Numerous studies have been conducted on castellated columns and beams. The work includes the investigation of the flexural buckling of castellated columns under the action of axially compressive loads

(El-Sawy et al. 2009; Gu and Cheng 2016; Sonck and Belis 2016; Yuan et al. 2014), the lateral-torsional buckling (Kim et al. 2016; Mohebkhah 2004; Nethercot and Kerdal 1982; Showkati et al. 2012; Sonck et al. 2014) and lateral buckling (Pattanayak and Chesson 1974; Sweedan 2011) of castellated beams when subjected to transverse loads, the shear buckling (Wang et al. 2014; Wang et al. 2016) and distortional buckling (Zirakian and Showkati 2006) of web-posts of castellated beams when there exist moment gradients, and the interaction of different buckling modes (Ellobody 2011; Kerdal and Nethercot 1984). In addition, geometrical and material nonlinear analyses using finite element methods (Mohebkhah and Showkati 2005; Soltani et al. 2012; Van Oostrom and Sherbourne 1972) and structural optimization (Gandomi et al. 2011; Gholizadeh et al. 2011; Najafi and Wang 2017; Sorkhabi et al. 2014; Tsavdaridis and D'Mello 2012) using numerical methods, neural networks and genetic programming have been also carried out in order to more accurately predict the structural behaviour of castellated members and improve their performance.

The aforementioned literature review shows that there have been extensive studies on the castellated columns and beams; the work includes both the analysis and design. However, limited work exists on the dynamics, particularly the dynamic instability of the castellated columns and/or beams when subjected to axial excitation loading. Note that the early work on the dynamic instability of elastic bodies was reported by Hsu (Hsu 1966), who investigated the dynamic instability of elastic body and presented corresponding necessary and sufficient stability criteria. Huang and Hung (Huang and Hung 1984) studied the dynamic instability of simply supported beams subjected to an axially periodic load using Routh-Hurwitz stability criteria and averaging method. The instability regions and vibration amplitudes were examined by considering the coupling of the first two modes. Park (Park 1987) presented a finite element dynamic instability model of Timoshenko beams, in which the transverse motion of the beam was expressed by using an extended Hamilton principle and the dynamic stability of the beams was investigated by examining the divergence and flutter instabilities. The results showed that the rotary inertia and shear deformation in certain ranges have significant effects on the stable transverse motion of the beams. Moreover, the dynamic instability of orthotropic beams (Huang 1980), thick bimodulus beams (Chen et al. 1991), and sandwich beams (Yeh et al. 2004) subjected to periodic axial loads has been also investigated by using the Bolotin method (Bolotin 1964). The effect of various different supporting boundary conditions on the dynamic instability behaviour of beams has been also examined and discussed, see (Kar and Sujata 1991; Uang and Fan 2001; Yoon and Kim 2002), for example.

This paper discusses the dynamic instability of castellated columns subjected to axial excitation loading. By assuming the instability modes, the kinetic energy and strain energy of the column and the loss of the potential of the axially compressive load are evaluated, from which the mass matrix, stiffness matrix, and geometric stiffness matrix of the system are derived. These matrices are then used for carrying out the analysis of dynamic instability by using Bolotin method. The analytical expressions for determining the critical excitation frequency of the columns are derived, which takes account for not only the shear influence of web openings but also the rotary inertia effect on the transverse vibration of the columns. Numerical examples are provided for illustrating the dynamic instability behaviour of castellated columns when subjected to axial excitation loading.

2. Brief description of dynamic instability analysis

The governing equation for the dynamic instability analysis of a structure when the damping is ignored can be expressed as follows (Kratzig et al. 1991; Li 1991; Patel et al. 2006),

$$[\mathbf{m}]\{\ddot{\mathbf{q}}\}+[\mathbf{k}]\{\mathbf{q}\}-P[\mathbf{k}_\mathbf{g}]\{\mathbf{q}\}=\{\mathbf{0}\} \tag{1}$$

where [**m**], [**k**], and [$\mathbf{k}_g$] are the mass matrix, stiffness matrix, and geometric stiffness matrix of the structural system, respectively, $\{\ddot{\mathbf{q}}\}$ is the column vector representing the acceleration vector, {**q**} is the column vector representing the displacement vector, and P is the externally applied load. If P = 0 then Eq.(1) represents the free vibration equation; whereas if the acceleration term is ignored then Eq.(1) represents the eigenvalue equation for linear buckling analysis. Assume that the externally applied load is a periodic one, in which case it can be expressed as follows,

$$P=\lambda P_{cr}\cos\Omega t \tag{2}$$

where λP_{cr} represents the amplitude of the dynamic load, P_{cr} is the critical buckling load for the case where the load is statically applied, λ is the loading factor, Ω is the excitation frequency of the dynamic load, and t is the time. For a given amplitude of the load the dynamic instability regions of the structure described by Eqs.(1) and (2) can be determined by examining the periodic solutions with the periods of $T=2\pi/\Omega$ and $2T=4\pi/\Omega$. The solution with the period of $2T$ is of particular importance, representing the primary instability region of the structure, which can be expressed using the form of trigonometric series given by Eq.(3),

$$\{\mathbf{q}\}=\sum_{k=1,3,\cdots}\left[\{\mathbf{a}_k\}\sin\frac{k\Omega t}{2}+\{\mathbf{b}_k\}\cos\frac{k\Omega t}{2}\right] \tag{3}$$

where $\{\mathbf{a}_k\}$ and $\{\mathbf{b}_k\}$ are the column-vectors of coefficients of the solution. Substituting Eqs.(2) and (3) into (1) and letting the coefficients of the series associated with $\sin(\Omega t/2)$ and $\cos(\Omega t/2)$ be zero, it yields,

$$\left([\mathbf{k}]+\frac{\lambda}{2}[\mathbf{k}_\mathbf{g}]-\frac{\Omega^2}{4}[\mathbf{m}]\right)\{\mathbf{a}_1\}=\{\mathbf{0}\} \tag{4}$$

$$\left([\mathbf{k}]-\frac{\lambda}{2}[\mathbf{k}_\mathbf{g}]-\frac{\Omega^2}{4}[\mathbf{m}]\right)\{\mathbf{b}_1\}=\{\mathbf{0}\} \tag{5}$$

Eqs.(4) and (5) are the generalized dynamic instability equations, which describe the resonance of a structure under the action of an excitation load. For a given value of λ, one can calculate two smallest positive frequencies of Ω; one is from Eq.(4) and the other is from Eq.(5), which represent the boundary of dynamic instability region of the structure.

3. Mass, stiffness, and geometric stiffness matrices of castellated columns

As reported in previous studies (El-Sawy et al. 2009; Gu and Cheng 2016; Yuan et al. 2014), web shear deformation has significant influence on the transverse displacement of castellated beam/columns. This means that the conventional Bernoulli's hypothesis can no longer be applied to the castellated beams/columns. Following the approach proposed by Yuan et al. (Yuan et al. 2014) and others (Chen et al. 2014; Gu 2014), the cross-sectional deformation of a castellated member is characterised in terms of three parts. One is the upper tee-section, one is the lower tee-section, and one is the mid part representing the discontinuous web posts, as illustrated in Fig.1. The axial displacements at the centroids of the two tee-sections are assumed to be independent. The axial displacement of the mid part is obtained by using linear interpolation between the two axial displacements defined at the tee-sections. The transverse displacements in all three parts are assumed to be identical. Moreover, it is assumed that the

two tee-sections deform according to Bernoulli's hypothesis, whereas the mid-part of the web posts behaves as a shear wall to take shear force only.

The stiffness matrix [**k**] of the castellated beam/column under an axial excitation load can be derived by using the energy method. Let u_1 and u_2 be the axial displacements of the dynamic buckling modal at the centroid points of the two tee-sections and v be the corresponding transverse displacement. The strain energy of the two tee-sections due to the dynamic buckling displacements can be expressed as follows,

$$U_1 = \frac{1}{2}\int_o^l \left[EA\left(\frac{du_1}{dx}\right)^2 + EA\left(\frac{du_2}{dx}\right)^2 + 2EI\left(\frac{d^2v}{dx^2}\right)^2 \right] dx \tag{6}$$

where E is the Young's modulus, A is the cross-sectional area of the tee-section, I is the second moment of area of the tee-section (about the centroid axis of the tee-section itself), and l is the length of the beam/column.

The shear strain energy of the discontinuous web posts (see Fig.1) is expressed as follows (Yuan et al. 2014),

$$U_2 = \frac{\sqrt{3}}{2} G t_w a^2 \sum \gamma_{xy}^2 \tag{7}$$

where G is the shear modulus, t_w is the web thickness, a is the half depth of hexagons, and γ_{xy} is the average shear strain of the mid-part of the web, which can be approximately expressed as follows,

$$\gamma_{xy} = \frac{e}{a}\frac{dv}{dx} - \frac{u_1 - u_2}{2a} \tag{8}$$

where e is the half distance between the centroids of the two tee-sections. Note that Eq.(7) is applied only to the castellated beam/column, in which the solid volume and void volume in the mid part are equal. Otherwise the pre-factor (1/2) in Eq.(7) has to be modified. Substituting Eq.(8) into (7) and using the assumption of smear model for the web posts, it yields,

$$U_2 = \frac{t_w e^2 G}{4a}\int_o^l \left(\frac{dv}{dx} - \frac{u_1 - u_2}{2e}\right)^2 dx \tag{9}$$

The geometric stiffness matrix [$\mathbf{k}_g$] of the castellated beam/column under an axial excitation of compressive load can be derived by using the potential change of the axially compressive load when the buckling occurs, which can be expressed as follows,

$$W = -P_{cr}\int_o^l \left[\frac{1}{2}\left(\frac{du_1}{dx} + \frac{du_2}{dx}\right) - \frac{1}{2}\left(\frac{dv}{dx}\right)^2 \right] dx \tag{10}$$

where P_{cr} is the critical buckling load.

The mass matrix [**m**] of the castellated beam/column can be derived using the kinetic energy of the beam/column. The kinetic energy of the two tee-sections due to axial and transverse vibrations are expressed as (Chen et al. 2014; Gu 2014),

$$T_1 = \frac{\rho A}{2}\int_o^l \left(\dot{u}_1^2 + \dot{u}_2^2\right) dx + \rho A\int_o^l \dot{v}^2 dx + \rho I\int_o^l \left(\frac{d\dot{v}}{dx}\right)^2 dx \tag{11}$$

where ρ is the density. The symbol with a dot above a variable represents the derivative of the variable with respect to time. The kinetic energy of the mid-part for the discontinuous web posts can be expressed as follows (Chen et al. 2014; Gu 2014),

$$T_2 = \frac{\rho a t_w}{2}\int_o^l \left(\frac{\dot{u}_1 + \dot{u}_2}{2}\right)^2 dx + \frac{\rho a t_w}{2}\int_o^l \dot{v}^2 dx + \frac{\rho a t_w}{6}\int_o^l \left(\frac{\dot{u}_1 - \dot{u}_2}{2} - (e-a)\frac{d\dot{v}}{dx}\right)^2 dx \tag{12}$$

Note that Eqs.(11) and (12) include also the kinetic energy due to the rotary inertia.

The axial and transverse displacements of the two tee-sections when the beam/column buckles dynamically can be assumed as follows,

$$u_1(x) = \frac{C_1 + C_2}{2}\cos\frac{\pi x}{l} \tag{13}$$

$$u_2(x) = \frac{C_1 - C_2}{2}\cos\frac{\pi x}{l} \tag{14}$$

$$v(x) = C_3 \sin\frac{\pi x}{l} \tag{15}$$

where C_1, C_2 and C_3 are the functions that depend only on time. Physically, C_1 and C_2 represent the average and difference of the axial displacements in the two tee-sections, respectively. It is obvious that the displacement functions assumed above have already satisfied the simply support boundary conditions, that is $v = dv^2/dx^2 = 0$, and $du_1/dx = du_2/dx = 0$ at both $x = 0$ and $x = l$. Substituting Eqs.(13)-(15) into (6) and (9), we obtain the stiffness matrix as follows:

$$[\mathbf{k}] = \begin{bmatrix} \frac{\partial^2(U_1+U_2)}{\partial C_1^2} & \frac{\partial^2(U_1+U_2)}{\partial C_1 \partial C_2} & \frac{\partial^2(U_1+U_2)}{\partial C_1 \partial C_3} \\ \frac{\partial^2(U_1+U_2)}{\partial C_2 \partial C_1} & \frac{\partial^2(U_1+U_2)}{\partial C_2^2} & \frac{\partial^2(U_1+U_2)}{\partial C_2 \partial C_3} \\ \frac{\partial^2(U_1+U_2)}{\partial C_3 \partial C_1} & \frac{\partial^2(U_1+U_2)}{\partial C_3 \partial C_2} & \frac{\partial^2(U_1+U_2)}{\partial C_3^2} \end{bmatrix} = \begin{bmatrix} k_{11} & 0 & 0 \\ 0 & k_{22} & k_{23} \\ 0 & k_{23} & k_{33} \end{bmatrix} \tag{16}$$

in which,

$$k_{11} = \frac{EAl}{4}\left(\frac{\pi}{l}\right)^2,\ k_{22} = \frac{EAl}{4}\left(\frac{\pi}{l}\right)^2 + \frac{Gt_w l}{16a},\ k_{23} = -\frac{\pi G t_w e}{8a},\ k_{33} = EIl\left(\frac{\pi}{l}\right)^4 + \frac{Gt_w e^2 l}{4a}\left(\frac{\pi}{l}\right)^2$$

Substituting Eqs.(13)-(15) into (10), we obtain the geometric stiffness matrix as follows:

$$[\mathbf{k}_g] = \begin{bmatrix} \frac{\partial^2 W}{\partial C_1^2} & \frac{\partial^2 W}{\partial C_1 \partial C_2} & \frac{\partial^2 W}{\partial C_1 \partial C_3} \\ \frac{\partial^2 W}{\partial C_2 \partial C_1} & \frac{\partial^2 W}{\partial C_2^2} & \frac{\partial^2 W}{\partial C_2 \partial C_3} \\ \frac{\partial^2 W}{\partial C_3 \partial C_1} & \frac{\partial^2 W}{\partial C_3 \partial C_2} & \frac{\partial^2 W}{\partial C_3^2} \end{bmatrix} = \begin{bmatrix} 0 & 0 & 0 \\ 0 & 0 & 0 \\ 0 & 0 & k_{g33} \end{bmatrix} \tag{17}$$

in which,

$$k_{g33} = \frac{P_{cr} l}{2}\left(\frac{\pi}{l}\right)^2$$

Substituting Eqs.(13)-(15) into (11) and (12), we obtain the mass matrix as follows:

$$[\mathbf{m}]=\begin{bmatrix} \dfrac{\partial^2(T_1+T_2)}{\partial\dot{C}_1^2} & \dfrac{\partial^2(T_1+T_2)}{\partial\dot{C}_1\partial\dot{C}_2} & \dfrac{\partial^2(T_1+T_2)}{\partial\dot{C}_1\partial\dot{C}_3} \\ \dfrac{\partial^2(T_1+T_2)}{\partial\dot{C}_2\partial\dot{C}_1} & \dfrac{\partial^2(T_1+T_2)}{\partial\dot{C}_2^2} & \dfrac{\partial^2(T_1+T_2)}{\partial\dot{C}_2\partial\dot{C}_3} \\ \dfrac{\partial^2(T_1+T_2)}{\partial\dot{C}_3\partial\dot{C}_1} & \dfrac{\partial^2(T_1+T_2)}{\partial\dot{C}_3\partial\dot{C}_2} & \dfrac{\partial^2(T_1+T_2)}{\partial\dot{C}_3^2} \end{bmatrix}=\begin{bmatrix} m_{11} & 0 & 0 \\ 0 & m_{22} & m_{23} \\ 0 & m_{23} & m_{33} \end{bmatrix} \tag{18}$$

in which, $m_{11}=\dfrac{\rho(2A+t_w a)l}{8}$, $m_{22}=\dfrac{\rho(6A+t_w a)l}{24}$, $m_{23}=-\dfrac{\pi\rho t_w a(e-a)}{12}$,

$$m_{33}=\frac{\rho(2A+t_w a)l}{2}+\rho Il\left(\frac{\pi}{l}\right)^2+\frac{\rho t_w a(e-a)^2 l}{6}\left(\frac{\pi}{l}\right)^2$$

Note that, although the formulas used for the strain energy, potential change and kinetic energy are the same as those used in previous studies (Yuan et al., 2014; Gu, 2014) the expressions of the stiffness matrix, geometric stiffness matrix and mass matrix derived herein are different from those provided in the previous studies because of the use of different displacement functions. For a given λ value, two Ω values can be calculated from the zero determinant as follows,

$$\left\|[\mathbf{k}]\pm\frac{\lambda}{2}[\mathbf{k_g}]-\frac{\Omega^2}{4}[\mathbf{m}]\right\|=0 \tag{19}$$

It can be found from the mass, stiffness, and geometric stiffness matrices shown in Eqs.(16)-(18) that the first row is not coupled with the second and third rows in the 3x3 matrix, indicating that C_1 is independent of C_2 and C_3. This implies that the transverse bending vibration of the beam is actually independent of its axial membrane vibration. Thus, the critical excitation frequencies can be calculated directly from the sub-matrix only related to C_2 and C_3, from which the following formula can be obtained,

$$\frac{\Omega^2}{4}=\frac{\left(m_{22}k_{33}^*+m_{33}k_{22}-2m_{23}k_{23}\right)-\sqrt{\left(m_{22}k_{33}^*+m_{33}k_{22}-2m_{23}k_{23}\right)^2-4\left(m_{22}m_{33}-m_{23}^2\right)\left(k_{22}k_{33}^*-k_{23}^2\right)}}{2\left(m_{22}m_{33}-m_{23}^2\right)} \tag{20}$$

where $k_{33}^*=k_{33}\pm\dfrac{\lambda}{2}k_{g33}$.

4. Dynamic instability of castellated columns

Herein three numerical examples are discussed, which represent the castellated columns with narrow, medium, and wide flanges, respectively. The half distance between the centroids of the two tee-sections, the area and the second moment of area of the tee-section of the castellated columns are calculated as follows,

$$e=\frac{b_f t_f\left(\dfrac{h_w+t_f}{2}\right)+t_w\left(\dfrac{h_w}{2}-a\right)\left(\dfrac{h_w+2a}{4}\right)}{b_f t_f+t_w\left(\dfrac{h_w}{2}-a\right)} \tag{21}$$

$$A=b_f t_f+\left(\frac{h_w}{2}-a\right)t_w \tag{22}$$

$$I = \frac{b_f t_f^3}{12} + b_f t_f \left(\frac{h_w + t_f}{2} - e \right)^2 + \frac{t_w}{12} \left(\frac{h_w}{2} - a \right)^3 + t_w \left(\frac{h_w}{2} - a \right) \left(e - \frac{h_w + 2a}{4} \right)^2 \quad (23)$$

where b_f and t_f are the width and thickness of the flange, and h_w is the web depth. The dimensions and corresponding cross-sectional properties of the three castellated columns discussed herein are provided in Table 1. The static critical buckling loads of the three castellated columns are calculated using the formula below (Yuan et al. 2014), which can be also derived from the present stiffness and geometric stiffness matrices:

$$P_{cr} = 2 \left(\frac{\pi}{l} \right)^2 \left(EI + \frac{e^2 EA}{1 + \frac{4\pi^2 EAa}{G t_w l^2}} \right) \quad (21)$$

Fig.2 shows the dynamic instability zones of the three castellated columns at two different lengths (4.85 m and 7.27 m), which are calculated by using Eq.(20). It can be seen from the figure that the width of the dynamic instability zone increases with increased loading factor. Also, it can be seen that, with the increase of the flange width, both of the two arms defining the dynamic instability zone move towards to high frequency side, but the right arm moves slightly faster than the left arm, indicating that the width of the dynamic instability zone also increases when the flange width becomes wide. Comparing Fig.2b with Fig.2a, one can observe that, with the increase of the column length, the resonance frequency decreases and the effect of the flange width on the dynamic instability zone increases.

The previous studies showed that the web shear deformation can affect the flexural buckling (El-Sawy et al. 2009; Yuan et al. 2014) and transverse vibration (Chen et al. 2014; Gu 2014) of short castellated columns/beams. In order to demonstrate that the web shear deformation has a similar effect on the dynamic instability zone, Fig.3 shows the comparison of the dynamic instability zones of the narrow flange castellated columns of two different lengths (4.85 m and 7.27 m) with and without considering the shear effect, in which the dynamic instability zone of the column without shear effect is calculated simply by using Eq.(20) but taking shear module G as an infinite large number. It is observed from Fig.3 that, when the shear effect is ignored, the dynamic instability zone moves towards to high frequency side and the width of the dynamic instability zone also increases. The change of the dynamic instability zone caused by the shear effect becomes more significant for the short column (4.85 m long) than for the long column (7.27 m long).

Figs.4 and 5 show the similar comparisons of the dynamic instability zones for the medium and wide flange castellated columns of two lengths, respectively. The main features demonstrated by these two figures are very much similar to those illustrated in Fig.3. However, by comparing Figs. 3, 4 and 5, one can clearly find that the shear effect on the dynamic instability zone becomes more significant when the flanges of the castellated column become wider, particularly for the short column. Figs. 3-5 also show that the dynamic instability zone is much wide in a short column than in a long column of the same section size.

The dynamic instability zones shown in Fig.2a and 2b or Figs.3-5 illustrate the interactive behaviour between the vibration and buckling of the column when it is subjected to a dynamic load. The former is related to the frequency of the dynamic load; whereas the latter is dependent on the amplitude of the dynamic load. The dynamic instability is more dangerous than ordinary resonance as it is characterised by exponential growth of the response amplitudes even in the

presence of damping. The two boundaries of each dynamic instability zone define the two resonance frequencies, in which the larger one reflects the effect of tension action and the smaller one reveals the effect of compression action. The difference between these two resonance frequencies increases very fast with the increased amplitude of the dynamic load. Therefore, it is very important to know the dynamic instability zone and how the dynamic load affects the dynamic instability zone for the design of columns subjected to harmonic loading.

5. Conclusions

An analytical solution has been developed in this paper for determining the dynamic instability zone of castellated columns when subjected to axial excitation loading. By assuming the instability modes, the kinetic energy and strain energy of the column and the loss of the potential energy of the axially compressive load are evaluated, from which the mass matrix, stiffness matrix, and geometric stiffness matrix of the system are derived. These matrices are then used for carrying out the analysis of dynamic instability of castellated columns. From the results obtained the following conclusions can be drawn:

(1) The dynamic instability zone of the castellated column will move towards to high frequency side and the corresponding width of the dynamic instability zone increases when its flanges become wide.

(2) The consideration of the shear effect in castellated columns results in a shaft of the dynamic instability zone to low frequency side and a reduction of the width of the dynamic instability zone.

(3) The effect of web shear deformation on the dynamic instability zone becomes more significant in the short column than in the long column, and in the wide flange column than in the narrow flange column.

References

Bolotin, V. V. (1964). The Dynamic Stability of Elastic Systems. San Francisco, CA, Holden-day, Inc.

Chen, J. K., Kim, B. & Li, L. Y. (2014). Analytical approach for transverse vibration analysis of castellated beams. International Journal of Structural Stability and Dynamics, **14**(3), 1–13.

Chen, L. Y., Lin, P. D. & Chen, L. W. (1991). Dynamic stability of thick bimodulus beams. Computers & Structures, **41**(2), 257-263.

El-Sawy, K., Sweedan, A. & Martini, M. (2009). Major-axis elastic buckling of axially loaded castellated steel columns. Thin-Walled Structures, **47**(11), 1295–1304.

Ellobody, E. (2011). Interaction of buckling modes in castellated steel beams. Journal of Constructional Steel Research, **67**(5), 814-825.

Gandomi, A. H., Tabatabaei, S. M., Moradian, M., Radfar, A. & Alavi, A. H. (2011). A new prediction model for the load capacity of castellated steel beams. Journal of Constructional Steel Research, **67**(7), 1096-1105.

Gholizadeh, S., Pirmoz, A. & Attarnejad, R. (2011). Assessment of load carrying capacity of castellated steel beams by neural networks. Journal of Constructional Steel Research, **67**(5), 770-779.

Gu, J. Z. (2014). Free vibration of castellated beams with web shear and rotary inertia effects. International Journal of Structural Stability and Dynamics, **14**(6), 1–10 (1450011).
Gu, J. Z. & Cheng, S. S. (2016). Shear effect on buckling of cellular columns subjected to axially compressed load. Thin-Walled Structures, **98**(Part B), 416-420.
Hsu, C. S. (1966). On dynamic stability of elastic bodies with prescribed initial conditions. International Journal of Engineering Science, **4**(1), 1-21.
Huang, J. S. & Hung, L. H. (1984). Dynamic stability for a simply supported beam under periodic axial excitation. International Journal of Nonlinear Mechanics, **19**(4), 287-301.
Huang, C. C. (1980). Dynamic stability of generally orthotropic beams. Fibre Science and Technology, **13**(3), 187-198.
Kar, R. C. & Sujata, T. (1991). Dynamic stability of a rotating beam with various boundary conditions. Computers & Structures, **40**(3), 753-773.
Kerdal, D. & Nethercot, D. A. (1984). Failure modes for castellated beams. Journal of Constructional Steel Research, **4**(4), 295-315.
Kim, B., Li, L. Y. & Edmonds, A. (2016) Analytical solutions of lateral-torsional buckling of castellated beams. International Journal of Structural Stability and Dynamics, **16**(8), 1-16 (1550044).
Kratzig, W. B., Li, L. Y. & Nawrotzki, P. (1991). Stability conditions for non-conservative dynamical systems. Computational Mechanics, **8**(3), 145-151.
Li, L. Y. (1991). Interaction of forced and parametric loading vibrations. Computers and Structures, **40**(3), 615-618.
Mohebkhah, A. (2004). The moment-gradient factor in lateral–torsional buckling on inelastic castellated beams. Journal of Constructional Steel Research, **60**(10), 1481-1494.
Mohebkhah, A. & Showkati, H. (2005). Bracing requirements for inelastic castellated beams. Journal of Constructional Steel Research, **61**(10), 1373-1386.
Najafi, M. & Wang, Y. C. (2017). Behaviour and design of steel members with web openings under combined bending, shear and compression. Journal of Constructional Steel Research, **128**, 579-600.
Nethercot, D. A. & Kerdal, D. (1982). Lateral-torsional buckling of castellated beams. The Structural Engineer, **60**, 53–61.
Park, Y. P. (1987). Dynamic stability of a free Timoshenko beam under a controlled follower force. Journal of Sound and Vibration, **113**(3), 407-415.
Patel, S. N., Datta, P. K. & Sheikh, A. H. (2006). Buckling and dynamic instability analysis of stiffened shell panels. Thin-Walled Structures, **44**(3), 321-333.
Pattanayak, U. C. & Chesson, E. (1974). Lateral instability of castellated beams. AISC Engineering Journal, **11**(3), 73-79.
Showkati, H., Ghazijahani, T. G., Noori, A. & Zirakian, T. (2012). Experiments on elastically braced castellated beams. Journal of Constructional Steel Research, **77**, 163-172.
Soltani, M. R., Bouchaïr, A. & Mimoune, M. (2012). Nonlinear FE analysis of the ultimate behaviour of steel castellated beams. Journal of Constructional Steel Research, **70**, 101-114.
Sonck, D. & Belis, J. (2016) Weak-axis flexural buckling of cellular and castellated columns. Journal of Constructional Steel Research, **124**, 91-100.
Sonck, D., Van Impe, R. & Belis, J. (2014). Experimental investigation of residual stresses in steel cellular and castellated members. Construction and Building Materials, **54**, 512-519.
Sorkhabi, R. V., Naseri, A. & Naseri, M. (2014). Optimization of the castellated beams by particle swarm algorithms method. APCBEE Procedia, **9**, 381-387.
Sweedan, A. M. I. (2011). Elastic lateral stability of I-shaped cellular steel beams. Journal of Constructional Steel Research, **67**(2), 151-163.

Tsavdaridis, K. D. & D'Mello, C. (2012). Optimisation of novel elliptically-based web opening shapes of perforated steel beams. Journal of Constructional Steel Research, **76**, 39-53.

Uang, C. M. & Fan, C. C. (2001). Cyclic stability criteria for steel moment connections with reduced beam section. Journal of Structural Engineering, **127**(9), 1021-1027.

Van Oostrom, J. & Sherbourne, A. N. (1972). Plastic analysis of castellated beams—II. Analysis and tests. Computers & Structures, **2**(1/2), 111-140.

Wang, P., Guo, K., Liu, M. & Zhang, L. (2016). Shear buckling strengths of web-posts in a castellated steel beam with hexagonal web openings. Journal of Constructional Steel Research, **121**, 173-184.

Wang, P., Wang, X. & Ma, N. (2014). Vertical shear buckling capacity of web-posts in castellated steel beams with fillet corner hexagonal web openings. Engineering Structures, **75**, 315-326.

Yeh, J. Y., Chen, L. W. & Wang, C. C. (2004). Dynamic stability of a sandwich beam with a constrained layer and electrorheological fluid core. Composite Structures, **64**(1), 47-54.

Yoon, S. J. & Kim, J. H. (2002). A concentrated mass on the spring unconstrained beam subjected to a thrust. Journal of Sound and Vibration, **254**(4), 621-634.

Yuan, W. B., Kim, B. & Li, L. Y. (2014). Buckling of axially loaded castellated steel columns. Journal of Constructional Steel Research, **92**, 40-45.

Zirakian, T. & Showkati, H. (2006). Distortional buckling of castellated beams. Journal of Constructional Steel Research, **62**(9), 863-871.

Table 1 Dimensions and properties of two castellated columns

Parameter	**Narrow section**	**Medium section**	**Wide section**
Web depth, h_w (mm)	400	400	400
Web thickness, t_w (mm)	15	15	15
Flange width, b_f (mm)	100	200	400
Flange thickness, t_f (mm)	10	10	10
Half depth of hexagons, a (mm)	140	140	140
Half distance between centroids of tee sections, e (mm)	188	194	199
Length of unit, $6a/\sqrt{3}$ (mm)	485	485	485
Area of tee section, A (cm^2)	19	29	49
Second moment of area of tee section, I (cm^4)	85.86	104.70	120.33

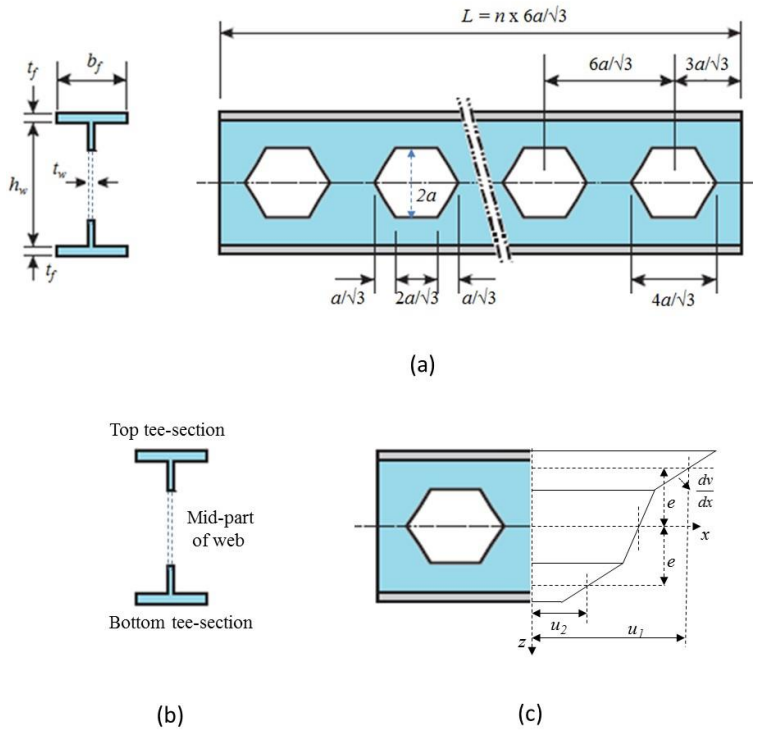

Figure 1. (a) Notations used for castellated column. (b) Section components. (c) Axial displacement distribution on cross-section.

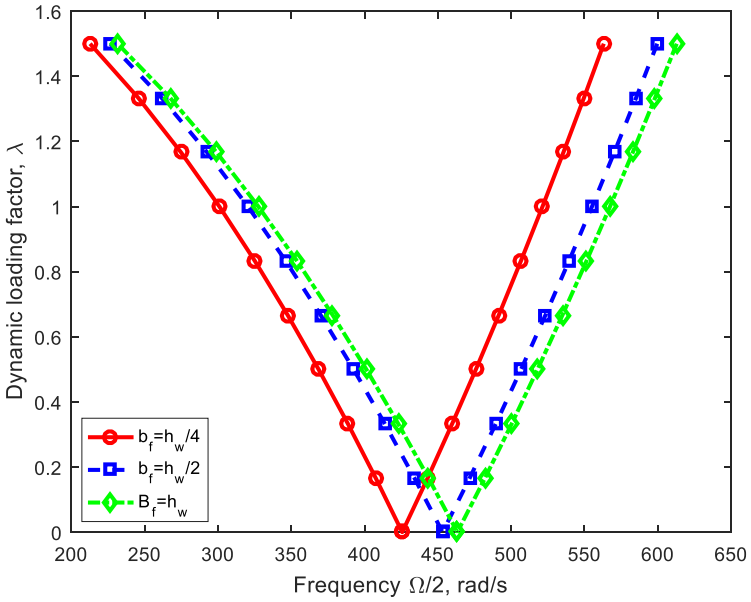

(a)

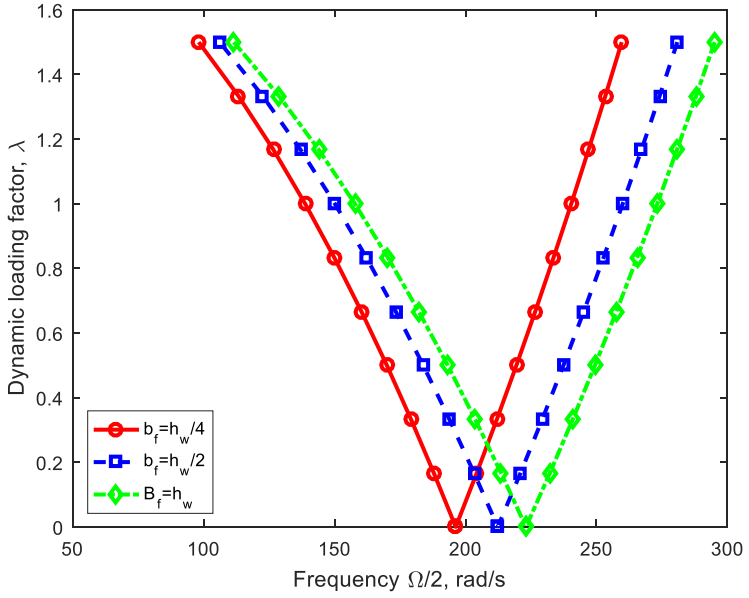

(b)

Figure 2. The dynamic instability zones of castellated columns with length (a) 4.85 m and (b) 7.27 m.

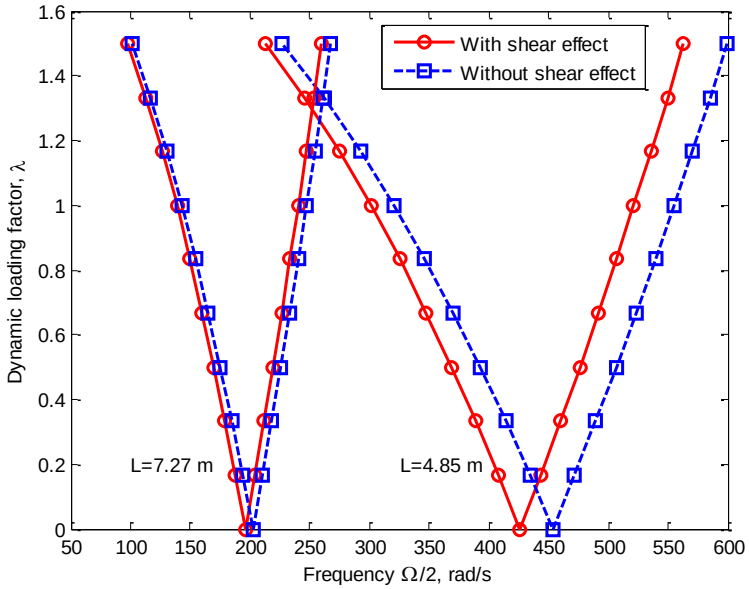

Figure 3. Shear effect on dynamic instability zone of castellated columns (b_w=100 mm).

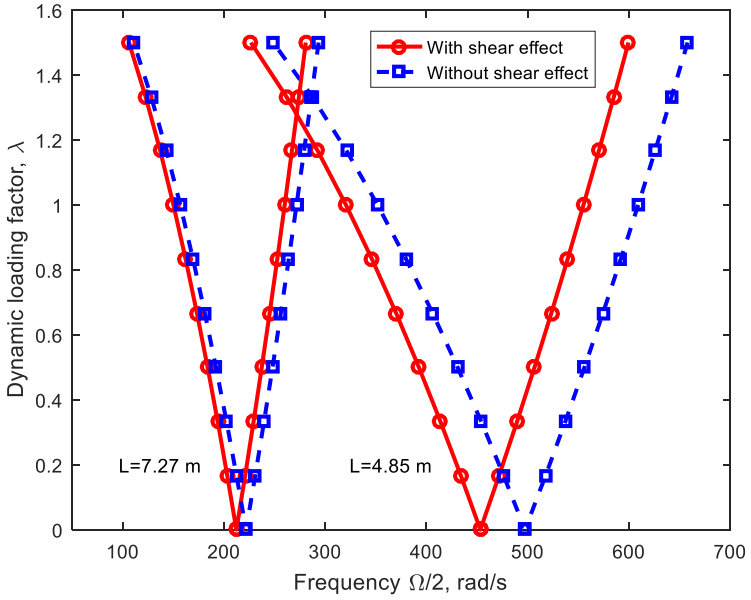

Figure 4. Shear effect on dynamic instability zone of castellated columns (b_w=200 mm).

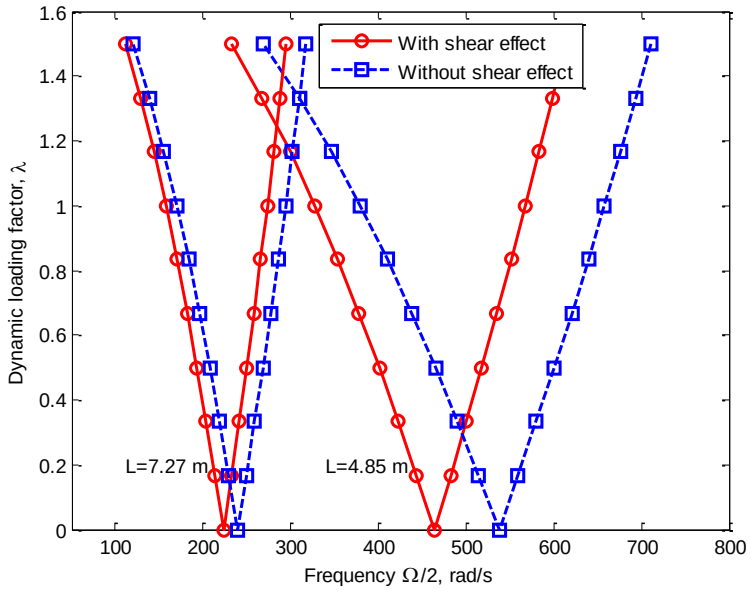

Figure 5. Shear effect on dynamic instability zone of castellated columns (b_w=400 mm).